

Golden Exosomes Selectively Target Brain Pathologies in Neurodegenerative and Neurodevelopmental Disorders

Nisim Perets,^{†,§,⊥} Oshra Betzer,^{‡,⊥} Ronit Shapira,^{||} Shmuel Brenstein,[†] Ariel Angel,[†] Tamar Sadan,[‡] Uri Ashery,^{†,||} Rachela Popovtzer,^{*,‡} and Daniel Offen^{*,†,§}

[†]Sagol School of Neuroscience, Tel Aviv University, Tel Aviv 6997801, Israel

[‡]Faculty of Engineering and the Institute of Nanotechnology and Advanced Materials, Bar-Ilan University, Ramat Gan 5290002, Israel

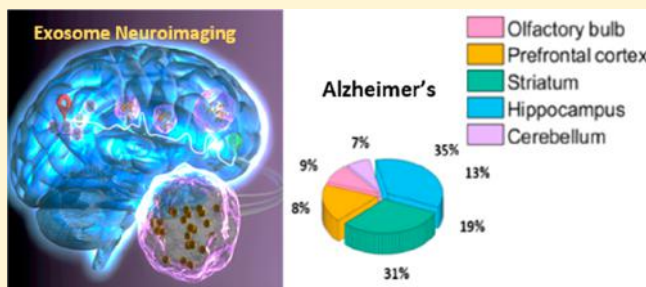
[§]Sacklar School of Medicine, Department of Human Genetics and Biochemistry, Tel Aviv University, Tel Aviv 6997801, Israel

^{||}School of Neurobiology, Biochemistry and Biophysics, Life Sciences Faculty, Tel Aviv University, Tel Aviv 6997801, Israel

Supporting Information

ABSTRACT: Exosomes, nanovesicles that are secreted by different cell types, enable intercellular communication at local or distant sites. Although they have been found to cross the blood brain barrier, their migration and homing abilities within the brain remain unstudied. We have recently developed a method for longitudinal and quantitative in vivo neuroimaging of exosomes based on the superior visualization abilities of classical X-ray computed tomography (CT), combined with gold nanoparticles as labeling agents. Here, we used this technique to track the migration and homing patterns of intranasally administrated exosomes derived from bone marrow mesenchymal stem cells (MSC-exo) in different brain pathologies, including stroke, autism, Parkinson's disease, and Alzheimer's disease. We found that MSC-exo specifically targeted and accumulated in pathologically relevant murine models brains regions up to 96 h post administration, while in healthy controls they showed a diffuse migration pattern and clearance by 24 h. The neuro-inflammatory signal in pathological brains was highly correlated with MSC-exo accumulation, suggesting that the homing mechanism is inflammatory-driven. In addition, MSC-exo were selectively uptaken by neuronal cells, but not glial cells, in the pathological regions. Taken together, these findings can significantly promote the application of exosomes for therapy and targeted drug delivery in various brain pathologies.

KEYWORDS: Exosomes, neuroimaging, gold nanoparticles, neuroinflammation, neurodegeneration, drug delivery



Development of targeted drug carriers is one of the greatest challenges for effective delivery of treatments for brain pathologies. Exosomes are emerging as potential carriers of therapeutics for such pathologies.^{1,2} These lipid nanovesicles (sized 40–150 nm), secreted by numerous cell types, serve as cell-to-cell communicators³ by transporting different proteins and nucleic acids with regulatory functions.⁴ Moreover, several studies have demonstrated that mesenchymal-derived and immune cell-derived exosomes cross the blood-brain barrier following systemic or intranasal administration with no need for surface modifications.^{1,5–8} We have recently shown that MSC-derived exosomes have a therapeutic effect on autistic-like behavior in the BTBR mouse model for autism.⁹ As compared to cell-based therapy, which shows promise for brain pathologies, and yet holds many risks, cell-derived exosomes have the advantage of lower immunogenicity, inability to proliferate, and simple preservation and transfer.¹⁰

The molecular features and regulatory and functional capacities of exosomes are mainly attributed to the type of cells from which they have been secreted.¹¹ Research shows that

mesenchymal stem cell (MSC)-derived exosomes (MSC-exo) retain some of the characteristics of their parent MSCs,^{4,12} such as immune system modulation,^{13,14} regulation of neurite outgrowth,^{15,16} promotion of angiogenesis,¹⁷ and the ability to repair damaged tissue, such as after kidney injury.^{18,19} An important question is whether MSC-exo also preserve the migration and homing abilities of parent MSCs.²⁰ Imaging of MSC migration in the brain has revealed specific homing to lesioned and diseased brain areas, such as in an ischemic stroke mouse model²¹ and an induced rat model of Huntington's disease,²² using magnetic resonance imaging, and in a genetic rat model for depression, using computed tomography (CT) imaging.^{23–25} It has been suggested that the therapeutic effect of MSCs on pathological regions is exerted via their secreted exosomes.²⁶

Received: October 16, 2018

Revised: February 10, 2019

Published: February 14, 2019

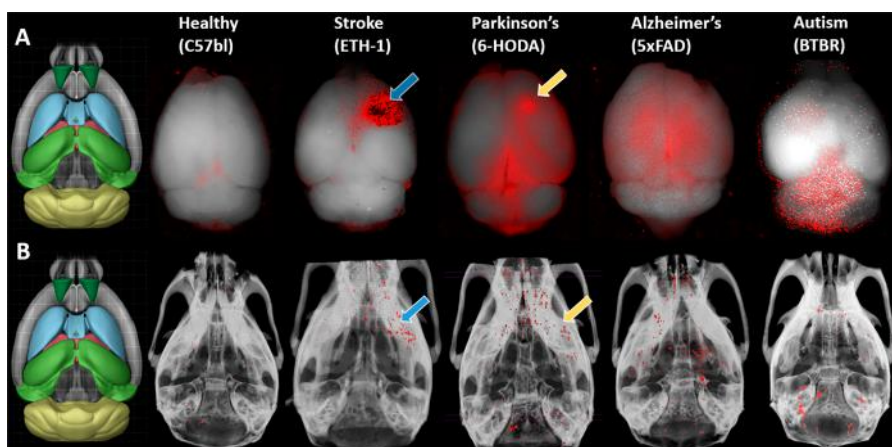


Figure 1. Differential distribution patterns of MSC-exo in various brain pathologies. (A) Ex vivo fluorescent imaging of PKH-26-labeled MSC-exo demonstrates different homing patterns in healthy controls, stroke, Parkinson's, Alzheimer's, and autism models, 24 h post intranasal administration. (B) In vivo CT imaging of GNP-loaded MSC-exo also demonstrates different homing patterns in healthy controls, stroke, Parkinson's, Alzheimer's, and autism, 24 h post intranasal administration, in concordance with the patterns visualized ex vivo. Blue arrow, location of ETH-1 injection; orange arrow, location of 6-OHDA injection. Relevant brain sections were adapted from the Allen Mouse Brain 3D Atlas (dark green, olfactory bulb; blue, striatum; red, thalamus; green, hippocampus; yellow, cerebellum).

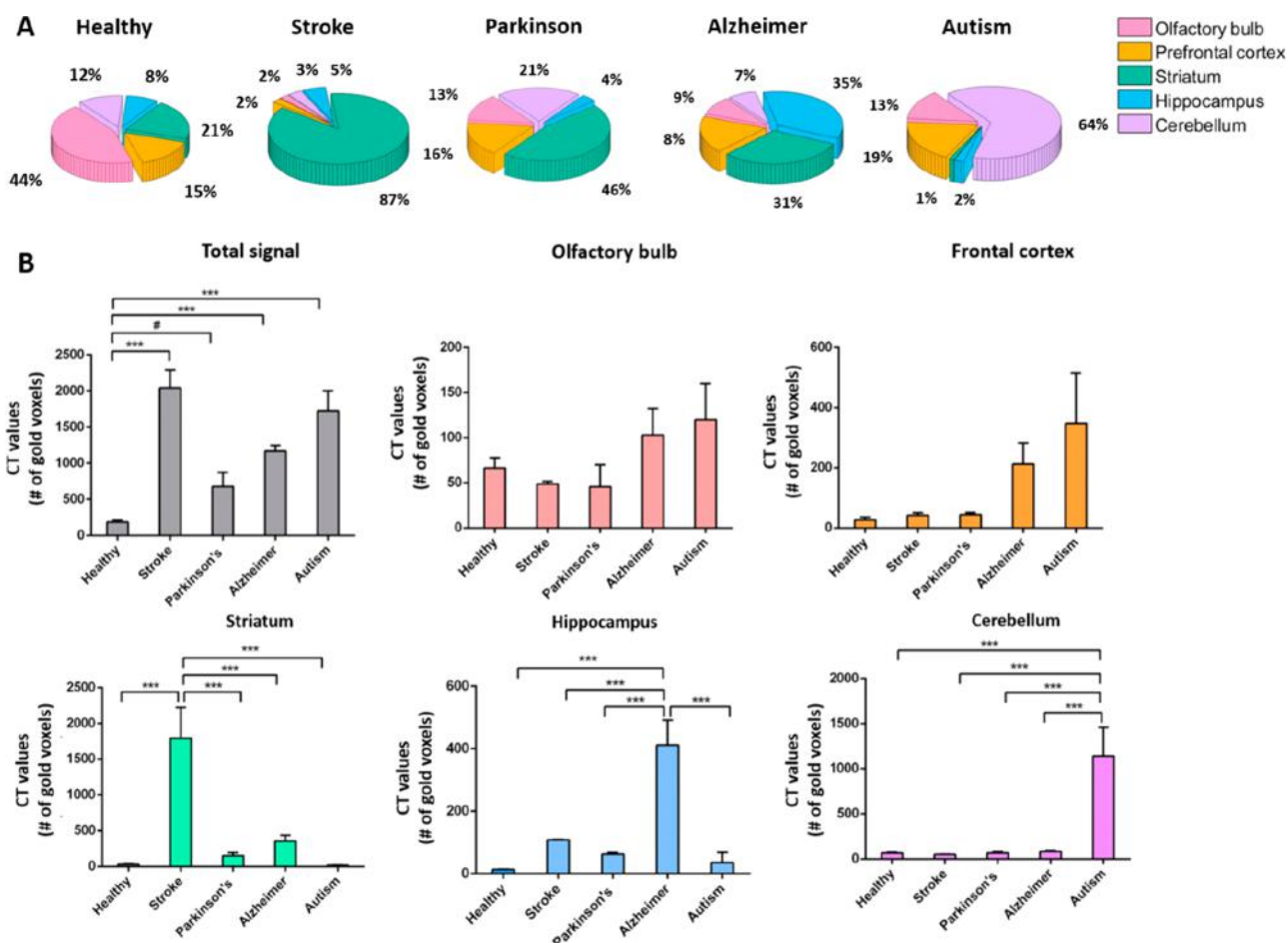


Figure 2. Quantitative comparison of CT values in the ROIs of different mouse models of brain pathologies. (A) Percentage of CT signal 96 h post administration is shown for healthy control mice, ETH-1 stroke model, 6-OHDA Parkinson's disease model, 5xFAD Alzheimer's disease model and BTBR autism model. Values are normalized to present percentiles according to the total number of gold voxels in each brain. (B) Comparison of CT value between the different models in the same brain area: olfactory bulb, frontal cortex, striatum, hippocampus, and cerebellum. Results presented as mean \pm SEM; #, trend toward significance; *** $p < 0.0001$.

Neuroinflammation, which plays a role in various brain pathologies,²⁷ is known to induce MSC migration.²⁸ Recent

work has demonstrated that neuroinflammation also triggers entry of macrophage-derived exosomes into the brain.²⁹

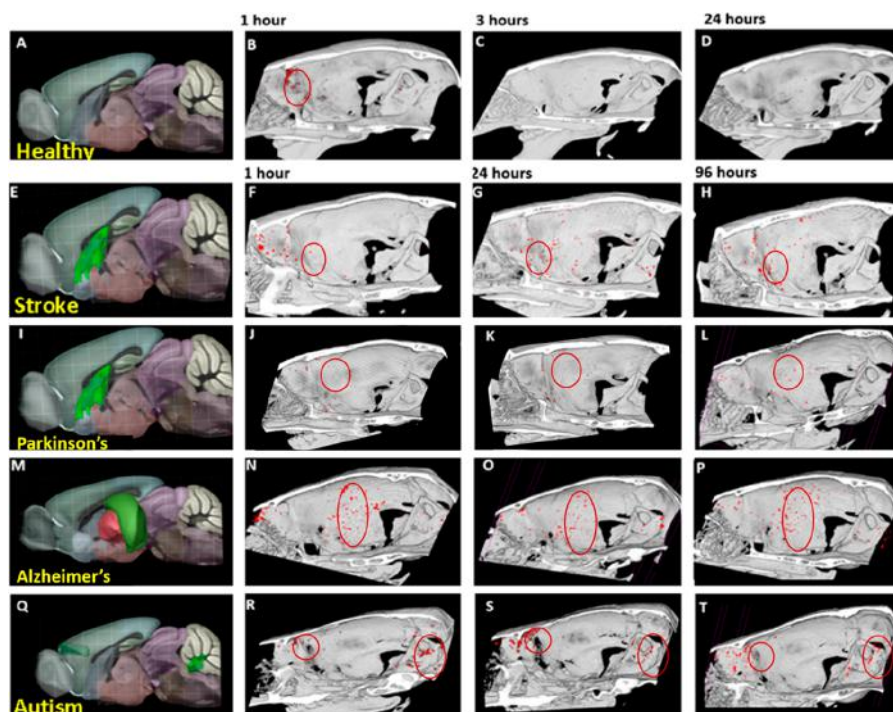


Figure 3. Longitudinal homing and accumulation of MSC-exo in diseased brains. (B–D) Healthy mice. CT signal, indicating presence of GNP-labeled MSC-exo, is found mainly in the olfactory bulb at 1 h and cleared by 24 h. (F–H) Stroke model. The MSC-exo CT signal was located in mouse striatum up to 96 h. (J–L) Parkinson’s disease model. MSC-exo signal was located in the striatum at 96 h. (N–P) Alzheimer’s model. MSC-exo signal was located in the hippocampus up to 96 h. (R–T) Autism model. MSC-exo signal was located in the cerebellum and prefrontal cortex up to 96 h. (A,E,I,M,Q) Brain section images adopted from Allen Mouse Brain 3D atlas, showing the lesioned/pathological area in green.

Furthermore, recent studies demonstrate that MSC-derived exosomes reduce neuroinflammation and promote neurogenesis and angiogenesis in status epilepticus animal models,³⁰ as well as rescue pattern separation and spatial learning impairments, and improve functional recovery, in animal models of traumatic brain injury.³¹

We have recently demonstrated migration of MSC-exo to a focal ischemic lesion site using a new *in vivo* exosome neuroimaging technique,³² combining gold nanoparticle (GNP) labeling^{33–38} and CT imaging.^{35,39} This noninvasive technique overcomes various limitations of exosome imaging in the brain, including the skull barrier and the exosomes’ nanosize, and enables whole-brain tracking and quantification of exosomes in specific brain regions.

In the present study, we longitudinally examined exosome migration and homing patterns in a range of induced, genetic, and inflammatory-associated murine models of brain pathologies, including neurovascular (ischemic stroke), neurodegenerative (Parkinson’s and Alzheimer’s disease), and neuropsychiatric (autism spectrum) disorders. GNP-labeled MSC-exo were intranasally administered, as this allows direct entry into the brain, bypassing the BBB,^{40,41} and as we have previously shown this to be an optimal route for brain accumulation.³² Migration was noninvasively tracked by CT up to 96 h. We demonstrate pathology-specific homing patterns of MSC-exo, which significantly correlated with pathology-associated neuroinflammation. Our data suggest that *in vivo* neuroimaging of MSC-exo can be used for diagnosis of brain deficiencies and further promote targeted drug delivery.

MSC-exo Present Distinct Distribution Patterns in Various Brain Pathologies. First, MSC-exo were loaded with glucose-coated GNPs according to our established protocol³²

(detailed procedures are available in [Supporting Information, Methods](#)). Nanosight and Western blot were used for MSC-exo characterization. Transmission electron microscope images confirmed particle internalization within the exosomes. (Exosome purification, GNPs synthesis and all characterization procedure details are included in [Supporting Information, Methods](#)). For particle and exosome characterization, see [Figures S1 and S2](#), and [SI Proteomics Assay File](#).

To determine distribution patterns of MSC-exo in various brain pathologies, we used several different mouse models, including models for focal ischemic stroke (via ETH1-1 injection),⁴² Parkinson’s disease (6-OHDA injection),^{43,44} Alzheimer’s disease (transgenic 5xFAD mice), and autism disorder (BTBR mice). MSC-exo presented distinct brain migration and homing patterns in each pathology, as shown both by *ex vivo* fluorescence imaging ([Figure 1A](#)) and *in vivo* CT imaging ([Figure 1B](#)). In the ischemic stroke model, MSC-exo migrated mainly to the injection area, in the striatal region. In the induced Parkinson’s model, a large amount of MSC-exo migrated to the striatal region but also to the midbrain and cerebellum, which are implicated in the disease as well.⁴⁵ In the Alzheimer’s model, MSC-exo were found mainly in the hippocampus, the central region associated with this disease.⁴⁶ In the autism model, *in vivo* and *ex vivo* imaging showed that MSC-exo homed to the cerebellum, and an additional CT signal was found in the prefrontal cortex; both regions are associated with autism.^{47,48} In healthy control brains, no CT or fluorescence signals were detected 24 h post administration, indicating clearance of MSC-exo from the brain.

Thus, *in vivo* CT imaging up to 24 h confirmed by fluorescence *ex vivo* imaging reveals that GNP-labeled MSC-exo accumulate only in pathological brains, and that the

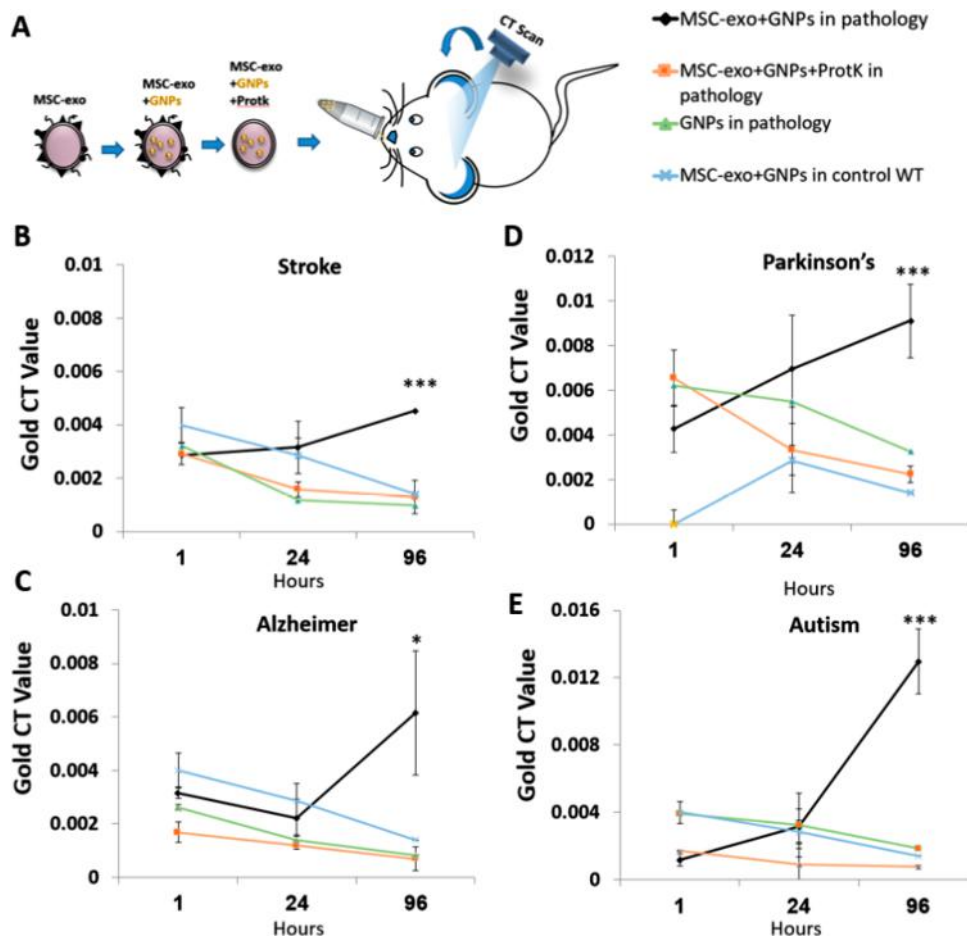


Figure 4. MSC-exo composition is crucial for increased homing in pathological brains. Mice in the different brain pathology models were treated with either MSC-exo, MSC-exo + protK, or GNPs. Gold values were examined in the whole brain and compared to that of healthy mice treated with MSC-exo. In all models, only MSC-exo showed an increased signal in the brain over time. (A) Schematic illustration showing preparation and administration of MSC-exo loaded with GNPs and treated with proteinase-k (protk). (B) Stroke model. (C) Parkinson's model. (D) Alzheimer's model. (E) Autism model. Gold CT value (for panels A–D) ≥ 66 ; (results presented as mean + SEM, * $p < 0.05$, *** $p < 0.0001$).

migration pattern is pathology-specific with homing to distinct pathology-related brain regions. Complete descriptions in vivo procedures are available in [Supporting Information](#), Methods.

Distribution Analysis of Pathology-Specific MSC-exo Homing. To analyze the distinct distribution patterns of GNP-labeled MSC-exo within pathological brains, CT signal intensity was noninvasively quantified (by number of gold voxels) in various regions of interest (ROI) (Figure 2). We show the percentage of distribution of GNP-labeled MSC-exo in each region, for each pathology (Figure 2A), and a comparison of the total voxel number in each region between the different pathologies (Figure 2B). It is notable that the total number of gold voxels in the pathological brains is significantly higher than in healthy mice, further indicating accumulation in the former versus clearance from the latter at 24 h (one way ANOVA $F(4,9) = 16.06$ $p < 0.001$, Tukey's post hoc).

For all mouse models, there was no significant difference between the CT values in the olfactory bulb, the area through which the exosomes entered the brain.

In the prefrontal cortex, a higher CT value, though not statistically significant, was found for the autism mice model as compared to the other disease models (one way ANOVA). In the striatum, mice with focal ischemic stroke showed a significantly higher CT value as compared to the other models (one way ANOVA, $F(4,9) = 40.8$ $p < 0.001$, Tukey's post hoc).

In the hippocampus, a significantly higher CT value was found for the Alzheimer's mouse model as compared to the other disease models (one way ANOVA $F(4,9) = 14.6$ $p < 0.001$, Tukey's post hoc). In the cerebellum, a significantly higher signal was found for the autism mouse model as compared to the other three models (one way ANOVA $F(4,9) = 8.41$ $p < 0.001$, Tukey's post hoc).

Taken together, the quantitative findings further support specific brain distribution and homing properties of MSC-exo in the different pathologies, as opposed to their clearance from the healthy brain.

Long-Term Brain Region Accumulation of MSC-exo in Different Pathologies. We next examined long-term migration and accumulation patterns of MSC-exo within the different brain pathologies up to 96 h. Mice of the four disease models and healthy controls ($n = 3$ /group/time point) received intranasal administration of GNP-labeled MSC-exo (2.8×10^9 exosomes, total volume of $20 \mu\text{L}$) and were CT scanned at 1, 24, and 96 h (Figure 3). In healthy mice, MSC-exo did not migrate beyond the olfactory bulb at 1 h post administration, and were gradually cleared 24 h later (Figure 3B–D). However, in the stroke model brain, MSC-exo were found at the striatal lesion at 1 h after injection and remained there up to 96 h (Figure 3F–H). In the Parkinson's model, MSC-exo were observed within the brain at 1 and 24 h, tending to a more widespread dispersal, and were

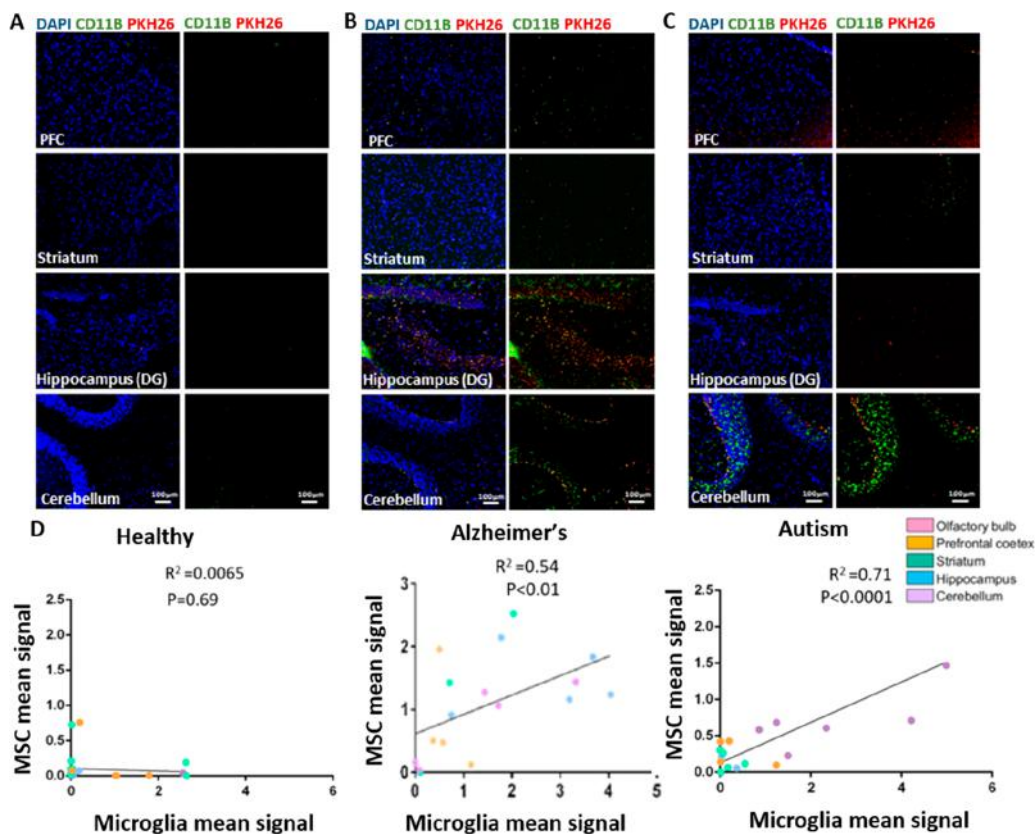


Figure 5. Immunostaining of neuro-inflammation and MSC-exo homing in brain regions. (A) Healthy control mice showed extremely low CD11b and PKH26 fluorescent signal in all examined regions. (B) Alzheimer's model mice showed a high CD11b signal in the hippocampus and striatum, and a relatively high signal in the frontal cortex and cerebellum, suggesting widespread neuro-inflammation. PKH26 signal was also relatively spread throughout the same areas. (C) Autism model mice showed high CD11b and PKH26 signals in the cerebellum but not in the other regions. (D) Correlation between CD11b and PKH26 fluorescent signals. Healthy controls showed low signals and no significant correlation between the two. Both Alzheimer's and autism model mice showed a significant correlation between CD11b and PKH26 intensities (note that the axes in the three graphs were fixed at $x = 5$ and $y = 3$ to compare between the disease models and healthy controls). Scale bar = 100 μm .

detected in the striatum region at 96 h (Figure 3J–L). In the Alzheimer's model, MSC-exo were located in the hippocampus between 1 and 96 h (Figure 3N–P), and in the autism model, they were found in the cerebellum and prefrontal cortex at 1–96 h (Figure 3R–T).

MSC-exo Accumulation Increases over Time and Is Membrane Protein-Composition Dependent. We subsequently examined accumulation rates of MSC-exo in the entire diseased brain over time and the possible role of exosome membrane proteins composition in the accumulation and migration process. Recent research reveals that membrane proteins of the coronal layer can significantly restrict or change exosome mobility.⁴⁹ We treated MSC-exo with proteinase-K (protK), a nonspecific serine endopeptidase which deconstructs proteins in their native state.⁵⁰ Nanosight measurements confirmed that the protK-treated exosomes were intact and uniform in size (Figure S6A). Mice of all four models ($n = 3$ /group) then received intranasal administration of either GNP-labeled MSC-exo, GNP-labeled MSC-exo treated with protK (MSC-exo+protK)^{15,32} (Figure 4A) or free GNPs. Healthy control mice were treated with GNP-labeled MSC-exo. CT scans were taken at 1, 24, and 96 h after treatment, and gold CT values were calculated in the whole brain. We found a gradual increase in gold CT values of MSC-exo over 96 h in all four mouse models while the values of control MSC-exo + protK, free GNPs, or MSC-exo in healthy mice, gradually decreased over

time. A statistically significant difference was found between the gold values of each pathology as compared to its controls at 96 h (one way ANOVA followed by Tukey's post hoc; ASD: $F(3,8) = 36.3386$, $p < 0.0001$, Post hoc, $p < 0.0001$. PD: $F(3,8) = 22.4137$; $p < 0.005$. Stroke: $F(3,8) = 27.7657$, $p < 0.0001$; $p < 0.0002$. AD: $F(3,8) = 4.8449$, $p < 0.03$; $p < 0.04$; Figure 4B–E; time course CT images of MSC-exo+protK and free GNPs are presented in Figures S4 and S5). Maestro imaging and histological staining showed protK-treated exosomes within the brain after 24 h, yet they were homogeneously dispersed in the brain, with no accumulation in pathological areas (Figure S6B,C). This indicates that the protK-treated exosomes retain the ability to cross the BBB, yet they do not target specific brain regions.

Moreover, to verify the specific ability of MSC-exo to migrate to diseased regions, Alzheimer's and autism mice were treated with control exosomes from primary myoblasts differentiated from MSCs (see Supporting Information, Methods). These control exosomes were almost undetectable in both brain types after 96 h (Figure S7), as opposed to the high and region-specific accumulation of the MSC-exo at this time point.

Taken together, these results further demonstrate and confirm that MSC-exo accumulate only in diseased brains and are gradually cleared from healthy brains and, importantly, that the unique protein composition of the MSC-exo membrane is crucial for their specific and long-term accumulation.

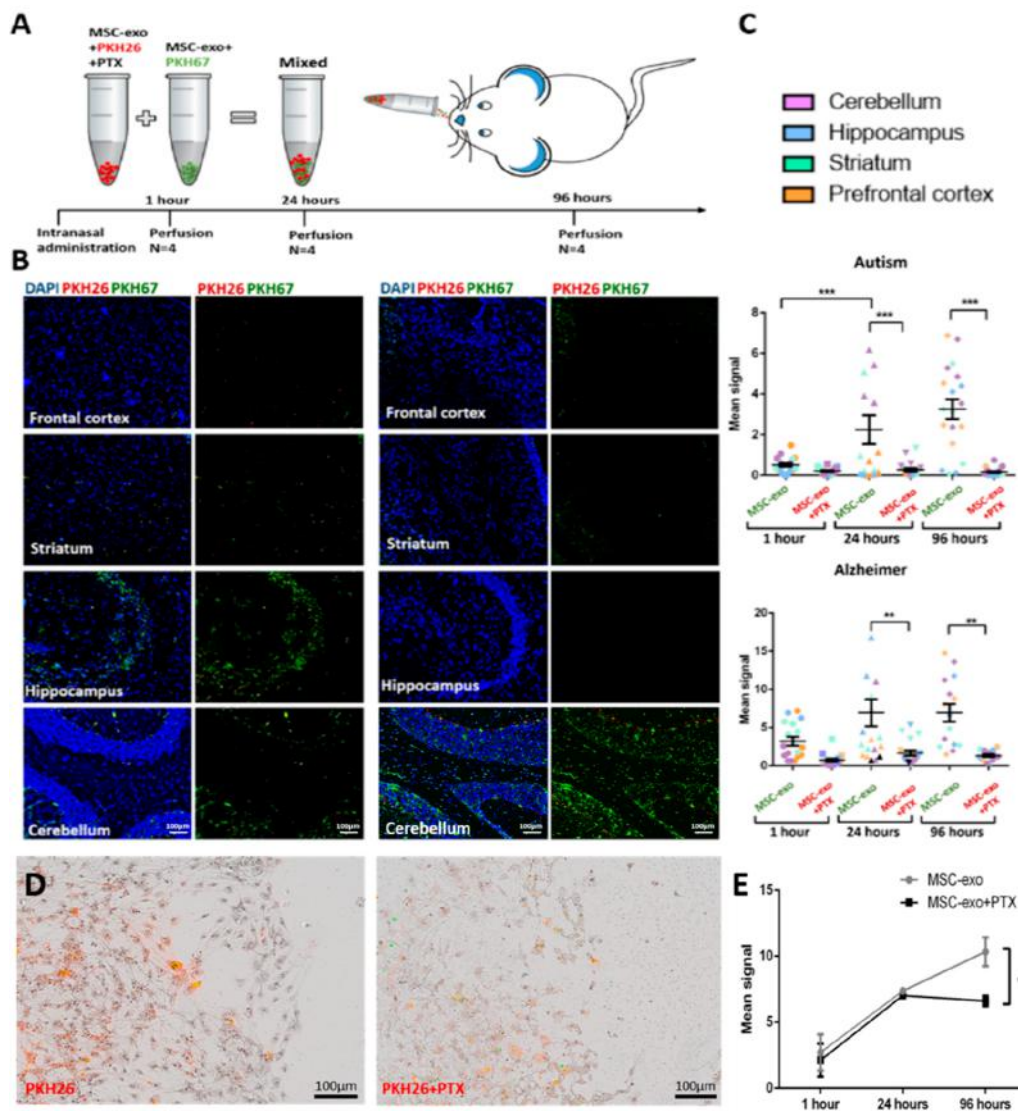


Figure 6. Immunostaining of MSC-exo and MSC-exo-PTX. (A) Experimental scheme, depicting MSC-exo labeled with PKH67 (green) and MSC-exo + PTX labeled with PKH26 (red), mixed and intranasally administered to Alzheimer's and autism mouse models. Mice were sacrificed 1, 24, or 96 h post administration. (B) Alzheimer's mice (left, 96 h) showed a high PKH-67 signal in the hippocampus, striatum, and cerebellum. PKH26 signal was low in all the measured regions. Autism mice (right, 96 h) showed a high PKH-67 signal in the cerebellum and frontal cortex. PKH26 signal was low in all the measured regions. (C) Quantification of mean fluorescence signal over time in the brain sections of the two mouse models shows increased PKH67 (green fluorescent signal) within 96 h and low PKH26 (red signal). (D) Primary culture of neurons with MSC-exo (left) and MSC-exo-PTX (right, 96 h post treatment) shows higher signal of MSC-exo compared to MSC-exo-PTX. (E) Time course quantification of MSC-exo and MSC-exo-PTX labeled with PKH26 in primary culture of neurons shows increase in signal after 24 h in both MSC-exo and MSC-exo-PTX and increased signal of MSC-exo but not MSC-exo+PTX after 96 h (results presented as mean + SEM, * $p < 0.05$, ** $p < 0.01$, *** $p < 0.001$). Analysis was conducted on the mean fluorescent signal in the green fluorescent channel compared to the red fluorescent channel of all samples at each time point. Scale bar = 100 μm .

MSC-exo Home to Inflammatory-Associated Regions in the Diseased Brain.

Neuroinflammation plays a role in various brain pathologies²⁷ and is associated with MSC migration.²⁸ Therefore, we next examined whether neuroinflammation in pathological brains can be associated with the specific MSC-exo migration. Alzheimer's and autism model mice were intranasally treated with PKH26-labeled MSC-exo (2.8×10^9 exosomes, total volume of 20 μL). Ninety-six hours later, brains were removed and sections from the frontal cortex, striatum, hippocampus and cerebellum were immunostained for CD11b, a marker of activated microglia,^{51,52} which are frequently found in inflammatory regions.⁵³ Immunostained cells were correlated with the PKH26 signal. In healthy mice, the anti-CD11b and PKH26 fluorescent signal intensity was low and

uncorrelated in all examined regions, indicating that no inflammation process had occurred and exosome migration was not targeted (Figure 5A,D). In Alzheimer's model mice, a high CD11b signal was observed, especially in the hippocampus and striatum, but also in the frontal cortex and cerebellum (Figure 5B). In autism model mice, a high CD11b signal was found in the cerebellum (Figure 5C). In both models, a significant correlation was found between CD11B and PKH26 signal intensities (Alzheimer's, $r^2 = 0.28$, $p < 0.05$; autism, $r^2 = 0.71$, $p < 0.01$; Figure 5D). These positive correlations indicate increased MSC-exo migration to regions of high inflammation and suggest that an inflammation-related mechanism, associated with the resident, innate immune microglia cells, underlies MSC-exo homing. Complete descriptions of fluorescent labeling

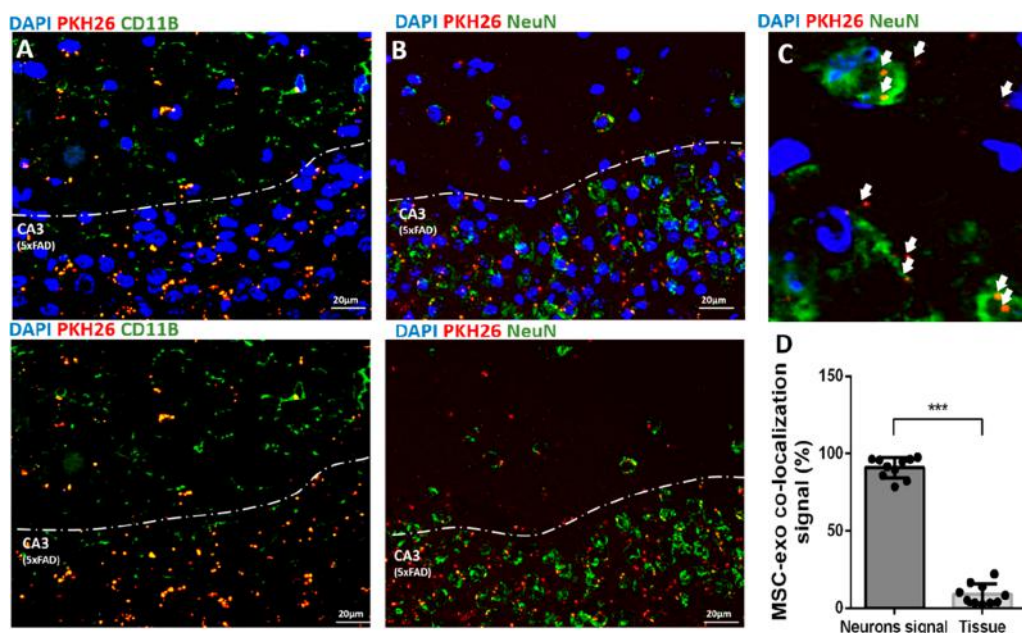


Figure 7. MSC-exo are uptaken by neurons in the pathological areas. (A). CD11b labeling of activated microglia in the CA3 hippocampal area of 5xFAD mice (top with DAPI, bottom without DAPI) shows MSC-exo homing to the neuronal layers of the CA3. (B) NeuN labeling of neurons in CA3 of 5xFAD mice (top with DAPI, bottom without DAPI) shows MSC-exo colocalized with neurons in CA3. (C) Magnification of neurons and other cells labeled with DAPI shows the large majority of MSC-exo within neurons with only a negligible amount external to the neurons in CA3. (D) Quantification of colocalization signal of MSC-exo and neurons in CA3. About 90% of the MSC-exo were found to be colocalized with neurons. (Results presented as mean + SD, *** $p < 0.001$.)

and ex-vivo procedures are available in [Supporting Information, Methods](#).

We further examined involvement of the innate immune response in migration of MSC-exo to specific pathology-related regions. We tested whether MSC-exo homing would be attenuated when using pertussis toxin (PTX). PTX modulates the innate immune response, leading to production of pro-inflammatory cytokines and inhibiting early chemotactic recruitment of macrophages and neutrophils;⁵⁴ it also blocks chemotactic-induced and malignant ascite-derived lysophosphatidic acid-induced, migration of MSCs.^{36,37}

Alzheimer's and autism model mice received an intranasal administration of a mixture of MSC-exo, labeled with PKH67 (green fluorescence; 5 μ l), and PTX-loaded MSC-exo (MSC-exo-PTX), labeled with PKH26 (red fluorescence). Mice were sacrificed at 1, 24, or 96 h post intranasal administration ($n = 3$ /group), and PKH26 and PKH67 signals were measured in the prefrontal cortex, striatum, hippocampus, and cerebellum (Figure 6A).

In Alzheimer's model mice, MSC-exo were found mainly in the hippocampus, as expected, with a gradual increase in accumulation over time, as seen by the increasing PKH67 signal, up to 96 h post administration. However, MSC-exo-PTX in Alzheimer's model mice showed significantly low accumulation, as seen by low PKH26 signal levels, in all brain areas and at all time points (one way ANOVA, $F(5,96) = 8.5$ $p < 0.0001$, Tukey's post hoc, $p < 0.001$). In the autism mouse model, a higher accumulation of MSC-exo, as seen by increased PKH67 signal, was seen mainly in the cerebellum and frontal cortex, while MSC-exo-PTX, denoted by PKH26 signal, was significantly low in all brain areas and all time points (one way ANOVA, $F(5,105) = 13.9$, $p < 0.0001$, followed by Tukey's post hoc, $p < 0.001$; Figure 6B,C). Thus, PTX inhibits specific

migration of MSC-exo in Alzheimer's and autism mouse model brains.

To confirm the effect of PTX on MSC-exo, a neuronal primary culture was prepared (see [Supporting Information, Methods](#)) and incubated (96 h) with either PKH26-labeled MSC-exo or PKH26-labeled MSC-exo-PTX. While the signal increased for both MSC-exo and MSC-exo-PTX at 24 h post treatment, it persisted only for MSC-exo with no increase for MSC-exo-PTX up to 96 h (Figure 6D; Figure 6E, one-way ANOVA $F(5,22) = 1.65$, Tukey post hoc).

Taken together, our findings suggest the involvement of an inflammation-associated innate immune response and possibly of chemotaxis-associated ligands upon the exosomes in MSC-exo homing.

MSC-exo Are Selectively Uptaken by Neurons in Pathological Regions. Following our finding that inflammation triggers region-specific exosome migration, we next examined which specific brain cell types were targeted by MSC-exo. Brain sections from the pathological regions of Alzheimer's mice treated with PKH26-labeled MSC-exo. Activated microglia were labeled with CD11b and neurons were labeled with NeuN for colocalization with PKH26-MSC-exo. In the hippocampus of Alzheimer's mice ($n = 3$, 4 samples each), approximately 90% of the MSC-exo signal was found in colocalization with the NeuN neuronal signal and not the microglial CD11b signal (Figure 7, paired t test $t(9) = 24.7$ $p < 0.001$). This finding indicates that MSC-exo specifically fuse with neurons, rather than microglia, at the target pathological region.

Taken together, our results indicate that inflammation triggers the exosome migration yet the target cells in the pathological regions are neurons.

Targeted drug delivery to injured brain regions remains an unmet challenge; this challenge is even more acute in

neuropsychiatric disorders, as the precise pathological location is often ambiguous. Exosomes are emerging as efficient delivery agents of therapeutics and molecular information to the brain.^{5,29,55} Their natural ability to cross the blood-brain barrier can be combined with noninvasive and highly effective intranasal administration,⁶ opening a new path for neurological and psychiatric medicine. The current study explored the migration and homing abilities of intranasally administered MSC-exo in a range of brain pathology models in mice, including induced stroke and induced Parkinson's model, a genetic Alzheimer's model, and a multifactorial autism model. Using our recently developed technique for *in vivo* neuroimaging of MSC-exo, we demonstrate a significant tendency of MSC-exo to migrate to specific pathology-related areas, and accumulate therein up to 96 h.

We have previously demonstrated the feasibility of our *in vivo* neuroimaging technology for detecting MSC-exo location within the brain in the induced ischemic stroke model up to 24 h,³² and in this work we found that MSC-exo can be detected in the ischemic brain up to 96 h. It is interesting to note that in both the induced stroke and PD models MSC-exo migrated to the lesioned striatum, yet in Parkinson's mice a relatively high signal was also observed in other areas such as the cerebellum.⁴⁵ These differences in homing patterns may indicate different spreading of the induced damage.^{45–48} The Alzheimer's model used here is based on five human genetic mutations on amyloid precursor protein (APP/PS1) genes, which lead to β -amyloid load in the hippocampus⁴⁶ and striatum.⁵⁶ Indeed, in these mice MSC-exo homing was found mainly in the hippocampus, as well as in the striatum. Autism spectrum disorders are considered one of the most challenging psychiatric disorders to diagnose, as the pathology cannot be pinpointed to a single factor or area of damage in the brain. As an autism mice model, we used BTBR mice, which show social interaction deficits, cognitive rigidity, and increased repetitive behaviors.^{48,57} We have recently shown that MSC-derived exosomes, but not neuronal stem cell-derived exosomes, have a therapeutic effect on autistic-like behavior in BTBR mice.⁹ Here, these mice showed the highest MSC-exo signal in the cerebellum, a region recently implicated in the disorder as shown by oxidative DNA damage and altered DNA methylation in both BTBR mice and post mortem analysis of human autistic brains.⁴⁷ A secondary signal of MSC-exo homing was found in the frontal cortex of BTBR mice;⁴⁸ indeed, deficits in this area have long been associated with autism, as established by post mortem studies.⁵⁸

Importantly, in all four brain pathology models, MSC-exo not only remained in the brain, but their accumulation in specific regions increased by 96 h; in healthy controls, MSC-exo were undetected after 24 h, indicating clearance from the brain. Additional control experiment with exosomes from primary myoblasts differentiated from MSCs showed that these control exosomes were almost undetectable in Alzheimer's and autism brains after 96 h, as opposed to the high and region-specific accumulation of the MSC-exo at this time point.

Inflammation has been suggested as one of the main factors that attracts MSC migration to lesioned tissues.⁵⁹ Activated microglia, resident innate immune cells which are found in areas of neuroinflammation, herein showed a significant correlation with MSC-exo homing; in addition, treatment with PTX, which inhibits key innate immune cells and promotes proinflammatory cytokine production,⁶⁰ blocked MSC-exo homing in models of Alzheimer's and autism. In our previous paper³² we ran *in vitro* tests for protK-treated GNP-loaded exosomes, and we found a

significantly lower uptake (over 80% reduction) level of protK-GNPs as compared to nontreated exosomes, indicating the involvement of exosome membrane proteins in active uptake pathways of the glucose-coated GNPs. In the current research, using *in vivo* pathological models, MSC-exo treated with protK were dispersed throughout the brain and did not accumulate at the inflammatory regions, as opposed to the nontreated MSC-exo. This implies that the migration pattern of the MSC-exo cannot be attributed to permeability of the inflammation region⁶¹ alone but to specific targeting to pathological regions.

In the Parkinson's model, we found a slower region-specific accumulation of MSC-exo (detected by CT after 96 h), which may be because the inflammation process in the induced 6-OHDA Parkinson's disease model, and microglia activation in particular, has a tendency to develop and increase over time.^{62,63}

BTBR mice have been shown to suffer from chronic neuroinflammation.⁶⁴ Interestingly, similarities in cerebellar dysfunctions, including increased neuroinflammation and altered methylation, were found between BTBR mice and post-mortem human autism brains.⁴⁷ Furthermore, in both SxFAD and Alzheimer's post-mortem patients, increased neuroinflammation was found, as demonstrated by activated microglia expressing CD11.⁶⁵

Altogether, we show that our nanoparticle-based imaging technique enables noninvasive, longitudinal neuroimaging and tracking of exosome distribution in the brain. Our data demonstrate that MSC-exo have remarkable migration and homing abilities toward specific areas of neuropathology, and specifically to neurons, and that inflammation plays a role in these homing mechanisms. Future studies will examine treatment efficacy of MSC-exo, either with or without additional drug cargo.

Our findings suggest that *in vivo* neuroimaging of MSC-exo can be used for diagnosis of neuronal deficiencies and further promote targeted drug delivery. Thus, the revelation of specific migration and homing abilities of MSC-exo in various pathologies can pave the way for their use as multifunctional theranostic agents.

■ ASSOCIATED CONTENT

📄 Supporting Information

The Supporting Information is available free of charge on the ACS Publications website at DOI: [10.1021/acs.nanolett.8b04148](https://doi.org/10.1021/acs.nanolett.8b04148).

Expanded materials and methods and supporting figures, including additional details about the experimental methods, characterization of the GNPs and the exosomes, control groups imaging, muscle-derived exosomes control experiment, exosomes treated with protK characterization and experimental results (PDF)

Full MSC-exo proteomics assay file (XLSX)

■ AUTHOR INFORMATION

Corresponding Authors

*(D.O.): Israel Office Phone: + 972-3-9376130. Lab: + 972-3-9376130. Email: danioffen@gmail.com.

*(R.P.): Email: rachela.popovtzer@biu.ac.il.

ORCID

Oshra Betzer: [0000-0002-4429-7024](https://orcid.org/0000-0002-4429-7024)

Author Contributions

¹N.P. and O.B. contributed equally to research

Notes

The authors declare no competing financial interest.

ACKNOWLEDGMENTS

This work was partially supported by the Israel Science Foundation ISF (749/14), by the Israel Science foundation Joint NSFC-ISF Research Grant (2533/17), The National Natural Science Foundation of China (51761145041), and by the Council for Higher Education Postdoctoral Fellowship for Outstanding Woman in Science for O.B. We would also like to thank the Brainboost program for supporting N.P. with a scholarship.

REFERENCES

- (1) Alvarez-Erviti, L.; Seow, Y.; Yin, H.; Betts, C.; Lakkh, S.; Wood, M. J. A. Delivery of siRNA to the Mouse Brain by Systemic Injection of Targeted Exosomes. *Nat. Biotechnol.* **2011**, *29* (4), 341–345.
- (2) Lai, R. C.; Wee, R.; Yeo, Y.; Hian, K.; Kiang, S. Exosomes for Drug Delivery — a Novel Application for the Mesenchymal Stem Cell. *Biotechnol. Adv.* **2013**, *31* (5), 543–551.
- (3) Zhou, H.; Yuen, P. S. T.; Pisitkun, T.; Gonzales, P. A.; Yasuda, H.; Dear, J. W.; Gross, P.; Knepper, M. A.; Star, R. A. Collection, Storage, Preservation, and Normalization of Human Urinary Exosomes for Biomarker Discovery. *Kidney Int.* **2006**, *69* (8), 1471–1476.
- (4) Baglio, S. R.; Rooijers, K.; Koppers-Lalic, D.; Verweij, F. J.; Pérez Lanzón, M.; Zini, N.; Naaijken, B.; Perut, F.; Niessen, H. W.; Baldini, N.; et al. Human Bone Marrow- and Adipose-Mesenchymal Stem Cells Secrete Exosomes Enriched in Distinctive miRNA and tRNA Species. *Stem Cell Res. Ther.* **2015**, *6* (1), 127.
- (5) Xin, H.; Li, Y.; Cui, Y.; Yang, J. J.; Zhang, Z. G.; Chopp, M. Systemic Administration of Exosomes Released from Mesenchymal Stromal Cells Promote Functional Recovery and Neurovascular Plasticity after Stroke in Rats. *J. Cereb. Blood Flow Metab.* **2013**, *33*, 1711–1715.
- (6) Zhuang, X.; Xiang, X.; Grizzle, W.; Sun, D.; Zhang, S.; Axtell, R. C.; Ju, S.; Mu, J.; Zhang, L.; Steinman, L.; et al. Treatment of Brain Inflammatory Diseases by Delivering Exosome Encapsulated Anti-inflammatory Drugs from the Nasal Region to the Brain. *Mol. Ther.* **2011**, *19* (10), 1769–1779.
- (7) Ha, D.; Yang, N.; Nadithe, V. Exosomes as Therapeutic Drug Carriers and Delivery Vehicles across Biological Membranes: Current Perspectives and Future Challenges. *Acta Pharm. Sin. B* **2016**, *6*, 1–10.
- (8) Haney, M. J.; Klyachko, N. L.; Zhao, Y.; Gupta, R.; Plotnikova, E. G.; He, Z.; Patel, T.; Piroyan, A.; Sokolsky, M.; Kabanov, A. V.; et al. Exosomes as Drug Delivery Vehicles for Parkinson's Disease Therapy. *J. Controlled Release* **2015**, *207*, 18–30.
- (9) Perets, N.; Hertz, S.; London, M.; Offen, D. Intranasal Administration of Exosomes Derived from Mesenchymal Stem Cells Ameliorates Autistic-like Behaviors of BTBR Mice. *Mol. Autism* **2018**, *9* (1), 57.
- (10) Vader, P.; Mol, E. A.; Pasterkamp, G.; Schiffelers, R. M. Extracellular Vesicles for Drug Delivery. *Adv. Drug Delivery Rev.* **2016**, *106*, 148–156.
- (11) Valadi, H.; Ekström, K.; Bossios, A.; Sjöstrand, M.; Lee, J. J.; Lötvall, J. O. Exosome-Mediated Transfer of MRNAs and MicroRNAs Is a Novel Mechanism of Genetic Exchange between Cells. *Nat. Cell Biol.* **2007**, *9* (6), 654–659.
- (12) Yu, B.; Zhang, X.; Li, X. Exosomes Derived from Mesenchymal Stem Cells. *Int. J. Mol. Sci.* **2014**, *15* (3), 4142–4157.
- (13) Kordelas, L. MSC-Derived Exosomes: A Novel Tool to Treat Therapy-Refractory Graft-versus-Host Disease. *Leukemia* **2014**, *28*, 970–973.
- (14) Jesus, S.; Soares, E.; Cruz, M. T.; Borges, O. Exosomes as Adjuvants for the Recombinant Hepatitis B Antigen: First Report. *Eur. J. Pharm. Biopharm.* **2018**, *133*, 1–11.
- (15) Zhang, Y.; Chopp, M.; Liu, X. S.; Katakowski, M.; Wang, X.; et al. Exosomes Derived from Mesenchymal Stromal Cells Promote Axonal Growth of Cortical Neurons. *Mol. Neurobiol.* **2017**, *54* (4), 2659–2673.
- (16) Xin, H.; Li, Y.; Buller, B.; Katakowski, M.; Zhang, Y.; Wang, X.; Shang, X.; Zhang, Z. G.; Chopp, M. Exosome-Mediated Transfer of miR-133b from Multipotent Mesenchymal Stromal Cells to Neural Cells Contributes to Neurite Outgrowth. *Stem Cells* **2012**, *30* (7), 1556–1564.
- (17) Zhang, H.; Liu, X.; Huang, S.; Bi, X.; Wang, H.; Xie, L.; Wang, Y.; Cao, X.; Lv, J.; Xiao, F.; et al. Microvesicles Derived from Human Umbilical Cord Mesenchymal Stem Cells Stimulated by Hypoxia Promote Angiogenesis Both In Vitro and In Vivo. *Stem Cells Dev.* **2012**, *21* (18), 3289–3297.
- (18) Borges, A. A.; Sinigaglia-coimbra, R.; Reis, L. A.; Borges, F. T.; Simo, M. J.; Schor, N. Bone Marrow-Derived Mesenchymal Stem Cells Repaired but Did Not Prevent Gentamicin-Induced Acute Kidney Injury through Paracrine Effects in Rats. *PLoS One* **2012**, *7* (9), e44092.
- (19) Zhou, Y.; Xu, H.; Xu, W.; Wang, B.; Wu, H.; Tao, Y.; Zhang, B.; Wang, M. Exosomes Released by Human Umbilical Cord Mesenchymal Stem Cells Protect against Cisplatin-Induced Renal Oxidative Stress and Apoptosis in Vivo and in Vitro. *Stem Cell Res. Ther.* **2013**, *4* (2), 34.
- (20) Fox, J. M.; Chamberlain, G.; Ashton, B. A.; Middleton, J. Recent Advances into the Understanding of Mesenchymal Stem Cell Trafficking. *Br. J. Haematol.* **2007**, *137* (6), 491–502.
- (21) Crabbe, A.; Vandeputte, C.; Dresselaers, T.; Sacido, A. A.; Verdugo Garcia, J. M.; Eyckmans, J.; Luyten, F. P.; Van Laere, K.; Verfaillie, C. M.; Himmelreich, U. Effects of MRI Contrast Agents on the Stem Cell Phenotype. *Cell Transplant* **2010**, *19* (8), 919–936.
- (22) Sadan, O.; Shemesh, N.; Barzilay, R.; Bahat-Stromza, M.; Melamed, E.; Cohen, Y.; Offen, D. Migration of Neurotrophic Factors-Secreting Mesenchymal Stem Cells toward a Quinolinic Acid Lesion as Viewed by Magnetic Resonance Imaging. *Stem Cells* **2008**, *26*, 2542–2551.
- (23) Betzer, O.; Schwartz, A.; Motiei, M.; Kazimirsky, G.; Gispan, I.; Danti, E. Nanoparticle-Based CT Imaging Technique for Longitudinal and Quantitative Stem Cell Tracking within the Brain: Application in Neuropsychiatric Disorders. *ACS Nano* **2014**, *9*, 9274–9285.
- (24) Schwartz, A.; Betzer, O.; Kronfeld, N.; Kazimirsky, G.; Cazacu, S.; Finniss, S. Therapeutic Effect of Astroglia-like Mesenchymal Stem Cells Expressing Glutamate Transporter in a Genetic Rat Model of Depression. *Theranostics* **2017**, *7* (10), 2690.
- (25) Betzer, O.; Meir, R.; Motiei, M.; Yadid, G.; Popovtzer, R. Gold Nanoparticle-Cell Labeling methodology for tracking Stem Cells within the brain. *Proc. SPIE* **2017**, *10077*, 100771F.
- (26) Liu, S.; Liu, D.; Chen, C.; Hamamura, K.; Moshaverinia, A.; Yang, R.; Liu, Y.; Jin, Y.; Shi, S. MSC Transplantation Improves Osteopenia via Epigenetic Regulation of Notch Signaling in Lupus. *Cell Metab.* **2015**, *22* (4), 606–618.
- (27) Rogers, J.; Mastroeni, D.; Leonard, B.; Joyce, J.; Grover, A. Neuroinflammation in Alzheimer's Disease and Parkinson's Disease: Are Microglia Pathogenic in Either Disorder? *Int. Rev. Neurobiol.* **2007**, *82* (07), 235–246.
- (28) Glenn, J. D.; Whartenby, K. A.; Glenn, J. D.; Whartenby, K. A.; Neu, D. Mesenchymal Stem Cells: Emerging Mechanisms of Immunomodulation and Therapy. *WJSC* **2014**, *6* (5), 526–539.
- (29) Yuan, D.; Zhao, Y.; Banks, W. A.; Bullock, K. M.; Haney, M.; Batrakova, E.; Kabanov, A. V. Biomaterials Macrophage Exosomes as Natural Nanocarriers for Protein Delivery to in Fl. *Biomaterials* **2017**, *142*, 1–12.
- (30) Long, Q.; Upadhyay, D.; Hattiangady, B.; Kim, D.-K.; An, S. Y.; Shuai, B.; Prockop, D. J.; Shetty, A. K. Intranasal MSC-Derived AI-Exosomes Ease Inflammation, and Prevent Abnormal Neurogenesis and Memory Dysfunction after Status Epilepticus. *Proc. Natl. Acad. Sci. U. S. A.* **2017**, *114* (17), E3536–E3545.
- (31) Yang, Y.; Ye, Y.; Su, X.; He, J.; Bai, W.; He, X. MSCs-Derived Exosomes and Neuroinflammation, Neurogenesis and Therapy of Traumatic Brain Injury. *Front. Cell. Neurosci.* **2017**, *11*, 1–12.

- (32) Betzer, O.; Perets, N.; Angel, A.; Motiei, M.; Sadan, T.; Yadid, G.; Daniel, O.; Popovtzer, R. In Vivo Neuroimaging of Exosomes Using Gold Nanoparticles. *ACS Nano* **2017**, *11*, 10883–10893.
- (33) Betzer, O.; Perets, N.; Barnoy, E.; Offen, D.; Popovtzer, R. Labeling and tracking exosomes within the brain using gold nanoparticles. *Proc. SPIE* **2018**, *1050618*, 44.
- (34) Popovtzer, R. Biomedical Applications of Gold Nanoparticles. *Nanomedicine (London, U. K.)* **2014**, *9* (13), 1903–1904.
- (35) Kim, J.; Chhour, P.; Hsu, J.; Litt, H. I.; Ferrari, V. A.; Popovtzer, R.; Cormode, D. P. Use of Nanoparticle Contrast Agents for Cell Tracking with Computed Tomography. *Bioconjugate Chem.* **2017**, *28* (6), 1581–1597.
- (36) Betzer, O.; Shilo, M.; Opochninsky, R.; Barnoy, E.; Motiei, M.; Okun, E.; Yadid, G.; Popovtzer, R. The Effect of Nanoparticle Size on the Ability to Cross the Blood-Brain Barrier: An in Vivo Study. *Nanomedicine* **2017**, *12* (13), 1533–1546.
- (37) Meir, R.; Betzer, O.; Motiei, M.; Kronfeld, N.; Brodie, C.; Popovtzer, R. Design Principles for Noninvasive, Longitudinal and Quantitative Cell Tracking with Nanoparticle-Based CT Imaging. *Nanomedicine* **2017**, *13* (2), 421–429.
- (38) Betzer, O.; Ankri, R.; Motiei, M.; Popovtzer, R. Theranostic Approach for Cancer Treatment : Multifunctional Gold Nanorods for Optical Imaging and Photothermal Therapy. *J. Nanomater.* **2015**, *16* (1), 381.
- (39) Motiei, M.; Dreifuss, T.; Betzer, O.; Panet, H.; Popovtzer, A.; Santana, J.; Abourbeh, G.; Mishani, E.; Popovtzer, R. Differentiating Between Cancer and Inflammation: A Metabolic-Based Method for Functional Computed Tomography Imaging. *ACS Nano* **2016**, *10*, 3469.
- (40) Pires, A.; Fortuna, A.; Alves, G.; Falcão, A. Intranasal Drug Delivery: How, Why and What For? *J. Pharm. Pharm. Sci.* **2009**, *12* (3), 288–311.
- (41) Jiang, Y.; Zhu, J.; Xu, G.; Liu, X.; Jiang, Y.; Zhu, J.; Xu, G.; Liu, X. Expert Opinion on Drug Delivery Intranasal Delivery of Stem Cells to the Brain Intranasal Delivery of Stem Cells to the Brain. *Expert Opin. Drug Delivery* **2011**, *8*, 623.
- (42) Durukan, A.; Tatlisumak, T. Acute Ischemic Stroke : Overview of Major Experimental Rodent Models, Pathophysiology, and Therapy of Focal Cerebral Ischemia. *Pharmacol., Biochem. Behav.* **2007**, *87*, 179–197.
- (43) Talanov, S. A.; Oleshko, N. N.; Tkachenko, M. N.; Sagach, V. F. Pharmacoprotective Influences on Different Links of the Mechanism Underlying 6-Hydroxydopamine-Induced Degeneration of Nigrostriatal Dopaminergic Neurons. *Neurophysiology* **2006**, *38* (2), 128–133.
- (44) Schober, A. Classic Toxin-Induced Animal Models of Parkinson's Disease : 6-OHDA and MPTP. *Cell Tissue Res.* **2004**, *318*, 215–224.
- (45) Hellmann, M. A.; Panet, H.; Barhum, Y.; Melamed, E.; Offen, D. Increased Survival and Migration of Engrafted Mesenchymal Bone Marrow Stem Cells in 6-Hydroxydopamine-Lesioned Rodents. *Neurosci. Lett.* **2006**, *395*, 124–128.
- (46) Eimer, W. A.; Vassar, R. Neuron Loss in the SXFAD Mouse Model of Alzheimer's Disease Correlates with Intraneuronal A β 42 Accumulation and Caspase-3 Activation. *Mol. Neurodegener.* **2013**, *8*, 2.
- (47) Shpyleva, S.; Ivanovsky, S.; De Conti, A.; Melnyk, S.; Tryndyak, V.; Beland, F. A.; James, S. J.; Pogribny, I. P. Cerebellar Oxidative DNA Damage and Altered DNA Methylation in the BTBR T+tf/J Mouse Model of Autism and Similarities with Human Post Mortem Cerebellum. *PLoS One* **2014**, *9* (11), e113712.
- (48) Meyza, K. Z.; Defensor, E. B.; Jensen, A. L.; Corley, M. J.; Pearson, B. L.; Pobbe, R. L. H.; Bolivar, V. J.; Blanchard, D. C.; Blanchard, R. J. The BTBR T+ Tf/J Mouse Model for Autism Spectrum Disorders-in Search of Biomarkers. *Behav. Brain Res.* **2013**, *251*, 25–34.
- (49) Skliar, M.; Chernyshev, V. S.; Belnap, D. M.; Sergey, G. V.; Al-Hakami, S. M.; Bernard, P. S.; Stijleman, I. J.; Rachamadugu, R. Membrane Proteins Significantly Restrict Exosome Mobility. *Biochem. Biophys. Res. Commun.* **2018**, *501* (4), 1055–1059.
- (50) Gheczy, N.; Kuchler, A.; Walde, P. Proteinase K Activity Determination with Beta-Galactosidase as Sensitive Macromolecular Substrate. *Anal. Biochem.* **2016**, *513*, 54–60.
- (51) Monje, M. L.; Toda, H.; Palmer, T. D. Inflammatory Blockade Restores Adult Hippocampal Neurogenesis. *Science* **2003**, *302* (5651), 1760–1765.
- (52) Murphy, Á. C.; Lalor, S. J.; Lynch, M. A.; Mills, K. H. G. Brain, Behavior, and Immunity Infiltration of Th1 and Th17 Cells and Activation of Microglia in the CNS during the Course of Experimental Autoimmune Encephalomyelitis. *Brain, Behav., Immun.* **2010**, *24* (4), 641–651.
- (53) Salter, M. W.; Stevens, B. Microglia Emerge as Central Players in Brain Disease. *Nat. Med.* **2017**, *23* (9), 1018–1027.
- (54) Bestebroer, J.; De Haas, C. J. C.; Van Strijp, J. A. G. How Microorganisms Avoid Phagocyte Attraction. *FEMS Microbiol. Rev.* **2010**, *34* (3), 395–414.
- (55) Braccioli, L.; Velthoven, C. Van; Heijnen, C. J. Exosomes : A New Weapon to Treat the Central Nervous System. *Mol. Neurobiol.* **2014**, *49* (1), 113–119.
- (56) Cho, W. H.; Park, J. C.; Chung, C. H.; Jeon, W. K.; Han, J. S. Learning Strategy Preference of SXFAD Transgenic Mice Depends on the Sequence of Place/Spatial and Cued Training in the Water Maze Task. *Behav. Brain Res.* **2014**, *273*, 116–122.
- (57) Perets, N.; et al. Long Term Beneficial Effect of Neurotrophic Factors Secreting Mesenchymal Stem Cells Transplantation in the BTBR Mouse Model of Autism. *Behav. Brain Res.* **2017**, *331*, 254–260.
- (58) Zilbovicius, M.; Garreau, B.; Samson, Y.; Remy, P.; et al. Delayed Maturation of the Frontal Cortex in Childhood Autism. *American journal of psychiatry* **1995**, *152*, 2.
- (59) Becker, A. De; Riet, I. Van. Homing and Migration of Mesenchymal Stromal Cells : How to Improve the. *WJSC* **2016**, *8* (3), 73–87.
- (60) Loch, C.; Coutte, L.; Mielcarek, N. The Ins and Outs of Pertussis Toxin. *FEBS J.* **2011**, *278* (23), 4668–4682.
- (61) Abbott, N. J. Inflammatory Mediators and Modulation of Blood – Brain Barrier Permeability. *Cell Mol Neurobiology* **2000**, *20* (2), 131–147.
- (62) Marinova-mutafchieva, L.; Sadeghian, M.; Broom, L.; Davis, J.; et al. Relationship between Microglial Activation and Dopaminergic Neuronal Loss in the Substantia Nigra: A Time Course Study in a 6-Hydroxydopamine Model of Parkinson's Disease. *J. Neurochem.* **2009**, *110*, 966–975.
- (63) Rodrigues, R. W. P.; Gomide, V. C.; Chadit, G. Astroglial and microglial reaction after a partial nigrostriatal degeneration induced by the striatal injection of different doses of 6-hydroxydopamine. *Int. J. Neurosci.* **2001**, *109*, 91.
- (64) Ahmad, S. F.; Ansari, M. A.; Nadeem, A.; Bakheet, S. A.; AL-Ayadhi, L. Y.; Attia, S. M. Toll-like Receptors, NF- κ B, and IL-27 Mediate Adenosine A2A Receptor Signaling in BTBR T+Itpr3tf/J Mice. *Prog. Neuro-Psychopharmacol. Biol. Psychiatry* **2017**, *79* (May), 184–191.
- (65) Heneka, M. T.; Carson, M. J.; Khoury, J. El; Landreth, G. E.; Brosseron, F.; Feinstein, D. L.; Jacobs, A. H.; Wyss-Coray, T.; Vitorica, J.; Ransohoff, R. M.; et al. Neuroinflammation in Alzheimer's Disease. *Lancet Neurol.* **2015**, *14* (4), 388–405.

NOTE ADDED AFTER ASAP PUBLICATION

This paper published ASAP on February 27, 2019 with an error in the affiliation list. The revised paper was reposted on March 14, 2019.